

Towards Solar Altitude Guided Scene Illumination

Samed Doğan, Maximilian Hoh, Nico Leuze, Nicolas R.-Peña, Alfred Schöttl
Dept. of Electrical Engineering and Information Technology
University of Applied Sciences Munich, 80335 Munich, Germany
Email: samed.dogan@hm.edu

Abstract—The development of safe and robust autonomous driving functions is heavily dependent on large-scale, high-quality sensor data. However, real-world data acquisition demands intensive human labor and is strongly limited by factors such as labeling cost, driver safety protocols and diverse scenario coverage. Thus, multiple lines of work focus on the conditional generation of synthetic camera sensor data. We identify a significant gap in research regarding daytime variation, presumably caused by the scarcity of available labels. Consequently, we present the solar altitude as global conditioning variable. It is readily computable from latitude-longitude coordinates and local time, eliminating the need for extensive manual labeling. Our work is complemented by a tailored normalization approach, targeting the sensitivity of daylight towards small numeric changes in altitude. We demonstrate its ability to accurately capture lighting characteristics and illumination-dependent image noise in the context of diffusion models.

I. INTRODUCTION

Diffusion models [1], [2] have emerged as a powerful class of generative models, capable of synthesizing data samples of arbitrary modality. They consequently gained significant traction within the autonomous driving domain, enabling generation of complex driving scenarios under controlled environments.

Large bodies of work focus on the realistic generation of synthetic camera [3], [4] or multi-modal data [5]–[7], rightfully addressing core problems such as coherent multi-view generation and multi-sensor alignment. However, given the extensive research effort in spatial scene control and cross-modal consistency, the aspect of accurate daytime representation remains largely unaddressed. One possible explanation is the lack of distinct labels to accurately and, in the sense of location, globally model the daytime. For instance, nuScenes [8], a dataset highly used in the training of State of the Art (SotA) generative sensor models, merely provides one coarse prompt level label “Night”. Another underexplored component is the limited discussion surrounding the reproducibility of the sensor hardware. Despite prior research incorporating camera intrinsics and extrinsics [3], [5], the temporal variations in sensor noise due to ambient light changes remain unaccounted for, further reinforcing the relevance of the problem introduced in this work.

We present a methodology that tackles previously outlined challenges and can be incorporated into existing setups in an orthogonal manner. First, we introduce the sun altitude as novel global light conditioning variable. To the best of our knowledge, we are the first to do so within the domain of autonomous driving. The sun position can directly be obtained

from the respective dataset as long as ego-pose and the time of capture are known, eliminating the need for external coarse labels. We discuss the non-linear behavior between sun movement and perceived light, especially during sunset and sunrise, and suggest a normalization approach that retains global structure and local variation within the scalar range. We further showcase the efficacy of the sun altitude as a surrogate variable in modeling perceived image noise. Due to its lightweight hardware requirements, we use textual inversion [9] as our preferred implementation method.

In short, our contributions are as follows:

- We introduce the task of daylight variation for generative camera sensor models in the context of autonomous driving.
- We present the sun altitude as one possible conditioning variable for global illumination and suggest a tailored normalization and encoding procedure that accounts for the non-linear relationship between conditioning and apparent brightness.
- We showcase the capability of altitude conditioned models in capturing not only global-lighting but also illumination-dependent noise characteristics.

II. RELATED WORK

A. Diffusion Models

Diffusion models, designed to learn some data distribution $q(\mathbf{x})$, fundamentally operate under a two-step probabilistic framework. The forward process gradually corrupts some input data $\mathbf{x}_0 \sim q(\mathbf{x}_0)$ with Gaussian noise over a series of T time steps, such that $\mathbf{x}_T \sim \mathcal{N}(\mathbf{0}, \mathbf{I})$. The reverse process consists of a learnable model that recovers \mathbf{x}_0 from \mathbf{x}_T by iterative denoising. In its canonical form, Denoising Diffusion Probabilistic Models (DDPMs) [1] define the forward process as a fixed discrete-time Markov chain of length T , and the reverse process as a series of denoising autoencoders $\epsilon_\theta(\mathbf{x}_t, t)$, predicting the added noise ϵ at time step $t \sim \mathcal{U}(\{1, \dots, T\})$. Latent Diffusion Models (LDMs) [10], a class of DDPMs, perform diffusion in the latent space, given some latent variable $\mathbf{z} = \mathcal{E}(\mathbf{x})$, where \mathcal{E}, \mathcal{D} is a pre-trained encoder-decoder pair, respectively. Including some conditioning \mathbf{c} of arbitrary modality, $\epsilon \sim \mathcal{N}(\mathbf{0}, \mathbf{I})$ and $\mathbf{z}_0 = \mathcal{E}(\mathbf{x}_0)$, the LDM training objective is defined as:

$$L_{LDM} := \mathbb{E}_{\mathbf{z}_0, \epsilon, t, \mathbf{c}} [\|\epsilon - \epsilon_\theta(\mathbf{z}_t, t, \mathbf{c})\|_2^2]. \quad (1)$$

Equation (1) is a simplified version of the variational lower bound discussed in [1].

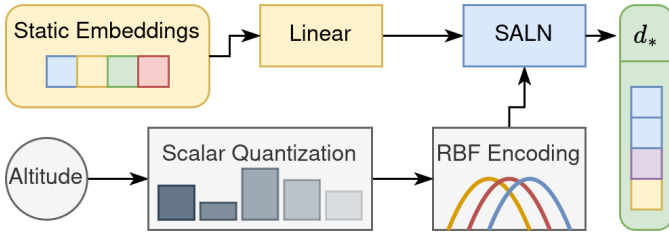


Fig. 1. Dynamic Embedding Pipeline

B. Textual Inversion

In general, text-to-image models employ a pre-trained text encoder in order to guide the image generation process towards some desired text prompt. A tokenizer maps the input prompt to a set of unique tokens on a per-word or sub-word basis. The discrete tokens index a corresponding learned embedding from an internal lookup table, forming the input embeddings. These are then further contextualized by the text encoder to capture sentence-level meaning. Textual inversion [9] is a prompt-based embedding technique that injects a new concept into the vocabulary of the text encoder by introducing a *pseudo-word* "V*" [11] that corresponds to a new learnable embedding v_* . The new embedding is trained to faithfully represent a given visual concept within the language domain of the diffusion model.

III. METHODOLOGY

A. Solar Altitude as Lighting Prior

Dataset Preparation. Assessing camera noise and natural lighting in non-controlled environments presents several key challenges: First, diffuse lighting conditions vary greatly over time and space. Second, we need to find a surrogate variable invariant to scene structure that accurately captures the relationship between illumination and noise. Assuming constant weather conditions, the solar altitude is a valuable proxy for the expected lighting characteristics and can thus serve as a strong surrogate measure of expected image noise. Following previous work [3], [5]–[7], we use nuScenes as exemplary dataset and filter samples containing the "Rain" label, as droplets on camera introduce heavy distortion. We convert the vehicle ego-pose to latitude and longitude coordinates and compute the sun altitude relative to the observer horizon using the astropy library [12].

Scalar Quantization with Residual Encoding. We observed a non-linear relationship between perceived light and sun position. More specifically, variation in solar altitude within sunset and sunrise windows lead to rapid shifts in illumination, whereas values around the zenith have negligible influence and are broadly overshadowed by weather and external conditions. Regular normalization procedures fall short of capturing fine variation, inevitably resulting in heavy semantic compression around sparse key regions. We draw inspiration from popular encoding schemes like positional [13] and Fourier encoding [14], aiming to preserve both coarse regions and fine grained

variation within the normalization range. Formally, given an increasing series of bin edges $b_0 < b_1 < \dots < b_K$ that define a range of intervals $[b_0, b_1), [b_1, b_2), \dots, [b_{K-1}, b_K)$, we first quantize the altitude $a \in \mathbb{R}$ such that $i = Q(a) := \max\{i \in \{0, \dots, K-1\} | b_i \leq a\}$. The residual function $R(a) \in [0, 1)$ captures the intra-bin variation, defined as the normalized offset of a within the bin i : $R(a) := \frac{a - b_i}{b_{i+1} - b_i}$. The normalized scalar \hat{a} is then obtained by:

$$\hat{a} = N(a) := \frac{Q(a) + R(a)}{K}. \quad (2)$$

We use an aggressive binning approach to mitigate the scarce availability of twilight and lack of sunrise samples. We further employ resampling with replacement, such that the bin count across all bins is approximately uniform. The explicit binning scheme is detailed in subsection IV-A.

B. Token Generation

Our method follows a two-stage process: first, we train a token that captures the general domain and visual composition of the camera images, hereafter referred to as structure token. Second, a separately trained conditional token captures the variation in daylight. We employ partial sampling similar to [15], [16] and use the context token during the first and the structure token during the second half of sampling.

Structure Token. Following [9], we learn a domain-specific word embedding s_* corresponding to the pseudo-word "S*". Let c_θ be a pre-trained CLIP [17] text encoder and y a text prompt. We omit the neural context text-templates from [9] and [17] during training, as we observed a degradation and overarching stylization of the camera data when used in unison. As a result, our training prompt y consists solely of "S*". The embedding s_* is obtained by freezing ϵ_θ and c_θ and directly optimizing the reconstruction objective of (1):

$$s_* = \arg \min_s \mathbb{E}_{\mathbf{z}_0, \epsilon, t, y} [\|\epsilon - \epsilon_\theta(\mathbf{z}_t, t, c_\theta(y))\|_2^2]. \quad (3)$$

We train s_* on the mini subset and explicitly exclude scenes at night to mitigate the impact of poor image quality on embedding performance.

Context Token. Contrary to the structure token, the embeddings d_* corresponding to "D*" are generated dynamically given the altitude a and a small network f_θ . To facilitate smoothness and localized sensitivity within the feature space, the scalar condition is first normalized according to (2) and enriched using an Radial Basis Function (RBF) encoding layer [18] with non-trainable uniformly placed centers and trainable gammas. We then use Style-Adaptive Layer Normalization (SALN) [19] to modulate a set of static embeddings based on the enriched input condition. A complete description of our network architecture is given in Fig. 1. The number of context embeddings are matched to that of the best structure embedding. We adopt the notation from (3) and train f_θ on the full dataset:

$$L_f := \mathbb{E}_{\mathbf{z}_0, \epsilon, t, y, a} [\|\epsilon - \epsilon_\theta(\mathbf{z}_t, t, c_\theta(y, f_\theta(a)))\|_2^2]. \quad (4)$$



Fig. 2. Comparison of ground truth samples (top) with generated images (bottom) across different input conditions of corresponding altitude (top). Conditions are normalized across the training bin range.

TABLE I
QUANTITATIVE RESULTS OF GENERATED IMAGES WITH VARYING SOLAR ALTITUDES. NORMALIZATION IS IDENTICAL TO FIG. 2. INCREMENTS $\Delta\sigma$ ARE COMPUTED FROM LEFT COLUMN TO RIGHT COLUMN.

Metric \ Altitude	0.0	0.33	0.66	1.0
FID (S*) ↓	—	—	—	151.433
FID (D* & S*) ↓	145.312	122.933	135.778	144.789
$\Delta\sigma$	—	-0.137	0.505	-1.223
$\Delta\sigma(\text{GT})$	—	-0.191	0.365	-1.389

IV. EXPERIMENTS

A. Implementation Details

We implement our method over Stable Diffusion (SD) 1.5 using the diffusers library [20]. All runs are trained for 5 epochs with a batch size of 8, a resolution of 224×400 and number of embeddings in the range [1, 5] using AdamW [21] with a weight decay of 0.01 and learning rates of $\{0.001, 0.005, 0.0001\}$. For evaluation, we sample a total of 64 images per prompt using the Denoising Diffusion Implicit Model (DDIM) [22] scheduler for 30 steps, a partial sampling step of 15 and Classifier-free Guidance (CFG) value of 7.5. Concerning normalization, we employ $[a_{\min}, -6, -4, -2, a_{\max}]$ as bin intervals, where a_{\min} and a_{\max} represent the smallest and largest available altitudes, respectively. If applicable, we advise a 2° step scheme from -12° (nautical twilight) to at least $+6^\circ$ (photographic golden hour).

B. Evaluation

Structure Token. Similar to [9], we use a dual score approach to assess the quality of latent space embeddings across different learning rates and number of tokens. In terms of visual fidelity, we compute the Fréchet Inception Distance (FID) between the training set and images generated using the prompt "S*". Regarding textual adherence, we measure the average cosine similarity of image and text embeddings in BLIP [23] space. Specifically, we generate images with "S* at night." and compare them with a variety of image

captions semantically close to "A traffic scene at night". The best performing embedding is picked for inference.

Context Token. The validation set does not contain samples captured during twilight conditions, rendering direct comparison infeasible. Instead, we evaluate the context token based on its ability to faithfully generate images across the provided altitude. We additionally measure the rate of change in estimated noise $\Delta\sigma$ using [24]. Ground truth data is filtered for back and front views. We complement the quantitative results in Table I with qualitative examples provided in Fig. 2.

V. CONCLUSION

In this work, we bring attention to current limitations in fine-grained control over scene illumination in the context of camera data generation. We hypothesize that the limited prior research is largely fueled by the constrained amount of relevant labels. To this end, we introduce the sun altitude as control variable, which can seamlessly be integrated as additional conditioning into existing diffusion frameworks. The computation is feasible in a fully automated manner with no reliance on manually labeled data, underscoring its scalability and potential for large-scale industrial datasets. We further suggest a tailored normalization approach that emphasizes numerical variation in regions of high perceptual sensitivity. Despite the very limited capacity of textual inversion, compounded by the scarcity of relevant data, our approach already shows very promising results. We are confident that integration into large-scale models will lead to further improvements in terms of precision and generalization. As such, we believe this work provides an additional stepping stone towards generating realistic and controllable camera data.

ACKNOWLEDGMENTS

The research leading to these results is funded by the German Federal Ministry for Economic Affairs and Energy within the project "NXT GEN AI METHODS – Generative Methoden für Perzeption, Prädiktion und Planung" (grant no. 19A23014M).

REFERENCES

- [1] J. Ho, A. Jain, and P. Abbeel, “Denoising diffusion probabilistic models,” *Advances in neural information processing systems*, vol. 33, pp. 6840–6851, 2020.
- [2] J. Sohl-Dickstein, E. Weiss, N. Maheswaranathan, and S. Ganguli, “Deep unsupervised learning using nonequilibrium thermodynamics,” in *Proceedings of the 32nd International Conference on Machine Learning*, ser. Proceedings of Machine Learning Research, F. Bach and D. Blei, Eds., vol. 37. Lille, France: PMLR, 07–09 Jul 2015, pp. 2256–2265. [Online]. Available: <https://proceedings.mlr.press/v37/sohl-dickstein15.html>
- [3] R. Gao, K. Chen, E. Xie, H. Lanqing, Z. Li, D.-Y. Yeung, and Q. Xu, “Magicdrive: Street view generation with diverse 3d geometry control,” in *The Twelfth International Conference on Learning Representations*, 2023.
- [4] A. Swerdlow, R. Xu, and B. Zhou, “Street-view image generation from a bird’s-eye view layout,” *IEEE Robotics and Automation Letters*, 2024.
- [5] Z. Wu, J. Ni, X. Wang, Y. Guo, R. Chen, L. Lu, J. Dai, and Y. Xiong, “Holodrive: Holistic 2d-3d multi-modal street scene generation for autonomous driving,” *arXiv preprint arXiv:2412.01407*, 2024.
- [6] Y. Xie, C. Xu, C. Peng, S. Zhao, N. Ho, A. T. Pham, M. Ding, M. Tomizuka, and W. Zhan, “X-drive: Cross-modality consistent multi-sensor data synthesis for driving scenarios,” *arXiv preprint arXiv:2411.01123*, 2024.
- [7] X. Wang, Z. Zhu, G. Huang, X. Chen, J. Zhu, and J. Lu, “Drivedreamer: Towards real-world-drive world models for autonomous driving,” in *European Conference on Computer Vision*. Springer, 2024, pp. 55–72.
- [8] H. Caesar, V. Bankiti, A. H. Lang, S. Vora, V. E. Liong, Q. Xu, A. Krishnan, Y. Pan, G. Baldan, and O. Beijbom, “nuscenes: A multimodal dataset for autonomous driving,” in *CVPR*, 2020.
- [9] R. Gal, Y. Alaluf, Y. Atzmon, O. Patashnik, A. H. Bermano, G. Chechik, and D. Cohen-or, “An image is worth one word: Personalizing text-to-image generation using textual inversion,” in *The Eleventh International Conference on Learning Representations*, 2023. [Online]. Available: <https://openreview.net/forum?id=NAQvF08TcyG>
- [10] R. Rombach, A. Blattmann, D. Lorenz, P. Esser, and B. Ommer, “High-resolution image synthesis with latent diffusion models,” in *Proceedings of the IEEE/CVF conference on computer vision and pattern recognition*, 2022, pp. 10 684–10 695.
- [11] N. Rathvon, *Early reading assessment*. New York, NY: Guilford Publications, Jun. 2004.
- [12] Astropy Collaboration, A. M. Price-Whelan, P. L. Lim, N. Earl, N. Starkman, L. Bradley, D. L. Shupe, A. A. Patil, L. Corrales, C. E. Brasseur, M. Nöthe, A. Donath, E. Tollerud, B. M. Morris, A. Ginsburg, E. Vaher, B. A. Weaver, J. Tocknell, W. Jamieson, M. H. van Kerkwijk, T. P. Robitaille, B. Merry, M. Bachetti, H. M. Günther, T. L. Aldcroft, J. A. Alvarado-Montes, A. M. Archibald, A. Bódi, S. Bapat, G. Barentsen, J. Bazán, M. Biswas, M. Boquien, D. J. Burke, D. Cara, M. Cara, K. E. Conroy, S. Conseil, M. W. Craig, R. M. Cross, K. L. Cruz, F. D’Eugenio, N. Dencheva, H. A. R. Devillepoix, J. P. Dietrich, A. D. Eigenbrot, T. Erben, L. Ferreira, D. Foreman-Mackey, R. Fox, N. Freij, S. Garg, R. Geda, L. Glattly, Y. Gondhalekar, K. D. Gordon, D. Grant, P. Greenfield, A. M. Groener, S. Guest, S. Gurovich, R. Handberg, A. Hart, Z. Hatfield-Dodds, D. Homeier, G. Hosseinzadeh, T. Jenness, C. K. Jones, P. Joseph, J. B. Kalmbach, E. Karamehmetoglu, M. Kałuszyński, M. S. P. Kelley, N. Kern, W. E. Kerzendorf, E. W. Koch, S. Kulumani, A. Lee, C. Ly, Z. Ma, C. MacBride, J. M. Maljaars, D. Muna, N. A. Murphy, H. Norman, R. O’Steen, K. A. Oman, C. Pacifici, S. Pascual, J. Pascual-Granado, R. R. Patil, G. I. Perren, T. E. Pickering, T. Rastogi, B. R. Roulston, D. F. Ryan, E. S. Rykoff, J. Sabater, P. Sakurikar, J. Salgado, A. Sanghi, N. Saunders, V. Savchenko, L. Schwardt, M. Seifert-Eckert, A. Y. Shih, A. S. Jain, G. Shukla, J. Sick, C. Simpson, S. Singanamalla, L. P. Singer, J. Singhal, M. Sinha, B. M. Sipócz, L. R. Spitler, D. Stansby, O. Streicher, J. Šumak, J. D. Swinbank, D. S. Taranu, N. Tewary, G. R. Tremblay, M. de Val-Borro, S. J. Van Kooten, Z. Vasović, S. Verma, J. V. de Miranda Cardoso, P. K. G. Williams, T. J. Wilson, B. Winkel, W. M. Wood-Vasey, R. Xue, P. Yoachim, C. Zhang, A. Zonca, and Astropy Project Contributors, “The Astropy Project: Sustaining and Growing a Community-oriented Open-source Project and the Latest Major Release (v5.0) of the Core Package,” *The Astrophysical Journal*, vol. 935, no. 2, p. 167, Aug. 2022.
- [13] A. Vaswani, N. Shazeer, N. Parmar, J. Uszkoreit, L. Jones, A. N. Gomez, Ł. Kaiser, and I. Polosukhin, “Attention is all you need,” *Advances in neural information processing systems*, vol. 30, 2017.
- [14] M. Tancik, P. Srinivasan, B. Mildenhall, S. Fridovich-Keil, N. Raghavan, U. Singhal, R. Ramamoorthi, J. Barron, and R. Ng, “Fourier features let networks learn high frequency functions in low dimensional domains,” *Advances in neural information processing systems*, vol. 33, pp. 7537–7547, 2020.
- [15] C. Mou, X. Wang, L. Xie, Y. Wu, J. Zhang, Z. Qi, and Y. Shan, “T2i-adapter: Learning adapters to dig out more controllable ability for text-to-image diffusion models,” in *Proceedings of the AAAI conference on artificial intelligence*, vol. 38, no. 5, 2024, pp. 4296–4304.
- [16] N. Ahn, J. Lee, C. Lee, K. Kim, D. Kim, S.-H. Nam, and K. Hong, “Dreamstyler: Paint by style inversion with text-to-image diffusion models,” in *Proceedings of the AAAI Conference on Artificial Intelligence*, vol. 38, no. 2, 2024, pp. 674–681.
- [17] A. Radford, J. W. Kim, C. Hallacy, A. Ramesh, G. Goh, S. Agarwal, G. Sastry, A. Askell, P. Mishkin, J. Clark *et al.*, “Learning transferable visual models from natural language supervision,” in *International conference on machine learning*. PmlR, 2021, pp. 8748–8763.
- [18] T. Poggio and F. Girosi, “Networks for approximation and learning,” *Proceedings of the IEEE*, vol. 78, no. 9, pp. 1481–1497, 1990.
- [19] D. Min, D. B. Lee, E. Yang, and S. J. Hwang, “Meta-stylespeech: Multi-speaker adaptive text-to-speech generation,” in *International Conference on Machine Learning*. PMLR, 2021, pp. 7748–7759.
- [20] P. von Platen, S. Patil, A. Lozhkov, P. Cuenca, N. Lambert, K. Rasul, M. Davaadorj, D. Nair, S. Paul, S. Liu, W. Berman, Y. Xu, and T. Wolf, “Diffusers: State-of-the-art diffusion models,” 2022. [Online]. Available: <https://github.com/huggingface/diffusers>
- [21] I. Loshchilov and F. Hutter, “Decoupled weight decay regularization,” *arXiv preprint arXiv:1711.05101*, 2017.
- [22] J. Song, C. Meng, and S. Ermon, “Denoising diffusion implicit models,” *arXiv preprint arXiv:2010.02502*, 2020.
- [23] J. Li, D. Li, C. Xiong, and S. Hoi, “Blip: Bootstrapping language-image pre-training for unified vision-language understanding and generation,” in *International conference on machine learning*. PMLR, 2022, pp. 12 888–12 900.
- [24] D. L. Donoho and I. M. Johnstone, “Ideal spatial adaptation by wavelet shrinkage,” *Biometrika*, vol. 81, no. 3, pp. 425–455, 09 1994. [Online]. Available: <https://doi.org/10.1093/biomet/81.3.425>